Naked mole rat brain mitochondria electron transport system flux and H^+ leak are reduced during acute hypoxia

Matthew E PAMENTER[1,2*], Gigi Y LAU[3], Jeffrey G RICHARDS[3], and William K MILSOM[3]

[1]Department of Biology, University of Ottawa, Ottawa, ON, CAN

[2]uOttawa Brain and Mind Research Institute, Ottawa, ON, CAN

[3]Department of Zoology, University of British Columbia, Vancouver, BC, CAN

Key words: cytochrome *c* oxidase, citrate synthase, proton gradient, mitochondrial membrane potential

Summary statement: The function of naked mole rat brain mitochondria is altered by hypoxia

Abbreviations: COX, cytochrome *c* oxidase; CS, citrate synthase; ETS, electron transport system; mtDNA, mitochondrial DNA; OGD, oxygen-glucose deprivation; $\Delta\Psi_m$, mitochondrial membrane potential; ROS, reactive oxygen species; SUIT, substrate-uncoupler-inhibitor titration; TPP, tetraphenylphosphonium;

[*]**Address for correspondence:** M. E. Pamenter, Ph.D. mpamenter@uottawa.ca

Abstract

Mitochondrial respiration and ATP production are compromised by hypoxia. Naked mole rats (NMRs) are among the most hypoxia-tolerant mammals and reduce metabolic rate in hypoxic environments; however, little is known regarding mitochondrial function during *in vivo* hypoxia exposure in this species. To address this knowledge gap, we asked whether the function of NMR brain mitochondria exhibits metabolic plasticity during acute hypoxia. Respirometry was utilized to assess whole-animal oxygen consumption rates and high-resolution respirometry and was utilized to assess electron transport system (ETS) function in saponin-permeabilized NMR brain. We found that NMR whole animal oxygen consumption rate reversibly decreased by ~ 85% in acute hypoxia (4 hrs at 3% O_2). Similarly, relative to untreated controls, permeabilized brain respiratory flux through the ETS was decreased by ~ 90% in acutely hypoxic animals. Relative to FCCP-uncoupled total ETS flux, this functional decrease was observed equally across all components of the ETS except for complex IV (cytochrome c oxidase), at which flux was further reduced, supporting a regulatory role for this enzyme during acute hypoxia. The maximum enzymatic capacities of ETS complexes I-V were not altered by acute hypoxia; however, the mitochondrial H^+-gradient decreased in step with the decrease in ETS respiration. Taken together, our results indicate that NMR brain ETS flux and H^+ leak are reduced in a balanced and regulated fashion during acute hypoxia. Changes in NMR mitochondrial metabolic plasticity mirror whole animal metabolic responses to hypoxia.

Introduction

Naked mole rats (NMRs; *Heterocephalus glaber*) are among the most hypoxia-tolerant mammals identified. In the laboratory, NMRs tolerate < 3% O_2 for several hours (Pamenter et al., 2014), 8% O_2 for days to weeks (Chung et al., 2016), and anoxia for up to 18 minutes (Park et al., 2017). This hypoxia-tolerance is likely the result of adaptations to the putatively hypoxic atmosphere in NMR burrows. Indeed, it is speculated that in the wild, given their deep nests and the large number of animals within the colony, that NMRs most likely encounter chronic hypoxia throughout their lives. Within their burrows, NMRs likely experience a gradient of hypoxic exposure, with the lowest level of O_2 occurring in the densely populated nest areas where the animals huddle in piles and sleep, and the lowest level of O_2 occurring at the extremes of the vast tunnel networks these animals dig in search of food, which can span many kilometers (Brett, 1991). Therefore, these animals likely experience intervals of acute and severe hypoxia while in their nest lasting for several hours.

NMRs exhibit a range of physiological adaptations that contribute to their hypoxia-tolerance, including a high-affinity hemoglobin (Johansen et al., 1976), the ability to metabolize alternative glycolytic substrates in anoxia (Park et al., 2017), dramatic reductions in metabolic rate and ventilation (Pamenter et al., 2015), and body temperature and behaviour(Kirby et al., In revision) in acute hypoxia, and metabolic remodeling in chronic hypoxia (Chung et al., 2016). Beyond systemic hypoxia-tolerance, there is also evidence that NMR brain is tolerant of low O_2 and even ischemic stresses *ex vivo*. For example, NMR brain slices retain synaptic activity in anoxia for up to 30 mins, tolerate O_2-glucose deprivation (OGD) for 24 hrs, and exhibit blunted neuronal Ca^{2+} influx during hypoxia (Nathaniel et al., 2009; Peterson et al., 2012). Conversely, hypoxia-intolerant murine brain slices tolerate only a few minutes of anoxia or OGD and exhibit large-scale deleterious Ca^{2+} influx during hypoxia (Nathaniel et al., 2009; Peterson et al., 2012).

In organisms that experience hypoxia, metabolic and cellular adaptations have evolved that scale to match a wide range of O_2 tensions. For example, reduced mitochondrial electron transport system (ETS) respiratory flux and/or adjustments to the H^+ gradient are commonly observed in isolated mitochondria from hypoxia- or anoxia-tolerant reptiles, amphibians, and invertebrates (Ali et al., 2012; Galli et al., 2013; Pamenter et al., 2016). Typically, this functional plasticity of mitochondria in hypoxia-tolerant species improves phosphorylation efficiency (*i.e.* ADP/O ratios) (St-Pierre et al., 2000; Pamenter, 2014). Mitochondria also coordinate neuroprotective responses against low O_2 stress in brains of hypoxia-tolerant species. For example, mitochondrial reactive oxygen species (ROS) generation and Ca^{2+} accumulation are regulated in anoxia-tolerant Western painted turtle [*Chrysemys picta bellii*] brains, and these signaling molecules in turn modulate neuronal membrane proteins and limit ion flux and deleterious neurotransmitter release. This prevents excitotoxic cell death during prolonged anoxia and ischemia (Pamenter et al., 2007; Pamenter et al., 2008; Pamenter et al., 2011; Pamenter et al., 2012; Hogg et al., 2015). Conversely, in brains of hypoxia-intolerant organisms, unregulated ROS generation and/or mitochondrial Ca^{2+} accumulation initiate cell death pathways during hypoxic or ischemic challenges (Choi, 1992; Pamenter, 2014). Therefore, mitochondria are at the center of neuronal energy production in normoxia and also the cellular decision between initiating neuroprotective responses *vs.* activating cell death cascades when O_2 is limited.

Despite the central role of mitochondria in cellular signaling during hypoxia and the prominence of NMRs as a mammalian model of hypoxia-tolerance, little is known about the function of NMR mitochondria outside of a few aging studies on muscle mitochondria that do not directly examine ETS function (Holtze et al., 2016; Stoll et al., 2016), while nothing is known regarding the effect of acute *in vivo* hypoxia on NMR brain mitochondrial ETS function. We hypothesized that brain mitochondria from NMRs exhibit metabolic plasticity in the form of altered

ETS flux and/or H^+ gradient kinetics following an acute hypoxic episode. We tested this hypothesis by exposing NMRs to 4 hrs of normoxia (21% O_2) or acute hypoxia (3% O_2) and examining the impact of this treatment on mitochondrial ETS flux. We found that NMR brain mitochondria exhibit a drastic 90% reduction in total ETS flux after acute *in vivo* hypoxic exposure, which closely matches the 85% whole animal oxygen consumption rate reduction observed during this hypoxic exposure.

Materials and Methodology

Animal husbandry and ethical Approval. All protocols were performed with the approval of The University of British Columbia Animal Care Committee. Animals were group-housed in interconnected multi-cage systems and held at 21% O_2 and 28°C in 50% humidity under a 12:12 h dim light-dark cycle. Animals were fed fresh tubers, vegetables, fruit, and Pronutro cereal supplement *ad libitum*. Animals were not fasted prior to experimental trials.

Whole animal respirometry. Adult male non-breeding NMRs (n = 16) were individually placed, unrestrained, into a 450 ml Plexiglas experimental chamber, which was set inside a controlled environmental chamber to maintain ambient temperature at ~ 28°C, which matched the housing temperature in the local animal care facility. The temperature of the animal chamber was recorded continuously using an iButton (Maxim Integrated, Chandler, CA). Calibrated rotameters were used to supply an inflowing gas mixture set at a flow rate of 110 ml•min^{-1}. The total airflow ensured that O_2 was not altered by more than 1.5% by the animal's metabolism. Fractional O_2 composition of inspired and expired gas was monitored using an O_2 analyzer (Raytech, North Vancouver, BC). The gas analyzer was calibrated before each trial with a premixed gas (21% O_2, balanced with N_2). O_2 consumption was calculated from the product of the constant airflow through the chamber and the difference in O_2 between the inflow and outflowing gasses. Whole animal oxygen consuption data

were recorded on WinDaq acquisition software (Dataq Instruments, Akron, OH), and analyzed in PowerLab. Once placed within the experimental apparatus, animals were given at least one hour to acclimate, and then metabolic measurements were collected for either 7 hrs in normoxia (21% O_2; control; n = 6) or one hour in normoxia following by 4 hrs in hypoxia (3% O_2; n = 10). All control animals were sacrificed following the normoxic protocol. Of the population of animals exposed to acute hypoxia, 6 animals were sacrificed for tissue sampling immediately following the hypoxic exposure, while 4 animals were permitted to recover in order to obtain recovery data for oxygen consuption rate.

Permeabilized brain mitochondrial preparation. Animals were sacrificed by cervical dislocation and whole brains were extracted over ice and bisected laterally within 30 secs. One half of each brain was frozen in liquid N_2 and stored at -80°C for enzyme analysis (see below); the other half was placed into ice-cold homogenization buffer (in mM: 250 sucrose, 10 TrisHCl, 0.5 Na_2EDTA; 1% fatty acid-free BSA, pH 7.4 at 4°C) and then minced over ice for 2-3 mins until the individual tissue pieces were uniformaly smaller than grains of sand. The resulting homogenate was permeabilized with 4 mM saponin in homogenization buffer for 45 mins, as described previously (Pamenter et al., 2016). Following permeabilization, the cell homogenate was re-suspended in ice-cold BIOPS medium (in mM: 10 Ca-K_2-EGTA, 5.8 NaATP, 6.6 $MgCl_2$, 20 imidazole, 20 taurine, 50 potassium 2-(N-morpholino)ethanesulfonic acid (K-MES), 15 Naphosphocreatine, 0.5 dithiothreitol (DTT); pH 7.1, adjusted with 5 N KOH), rinsed for 2 mins on ice, and then re-suspended in BIOPS medium. This rinse procedure was repeated 3 times. Permeabilized cells were kept on ice until use and all mitochondria were assayed within 2 hrs of isolation.

Mitochondrial respiration and membrane potential analysis. Permeabilized brain mitochondrial respiration was measured with an Oroboros Oxygraph 2-k high-resolution respirometry system (Oroboros Instruments, Innsbruck, Austria), as described previously (Galli et al., 2013). Two identical respiration chambers held at 28°C in parallel. Permeabilized brain cells were added to each chamber containing 2 ml of respiration solution (in mM: 0.5 EGTA, 1.4 $MgCl_2$, 20 taurine, 10 KH_2PO_4, 20 HEPES, 1% BSA, 60 K-lactobionate, 110 sucrose; pH 7.1, adjusted with 5 N KOH). Respiratory flux through the ETS was measured in permeabilized brain cells using a substrate-uncoupler-inhibitor-titration (SUIT) protocol described previously (Galli et al., 2013; Pamenter et al., 2016). State II respiration was used as a proxy for leak respiration because native ATPases prevent the establishment of steady state IV respiration in the saponin-permeabilized cell preparation. Respiration values were obtained from steady-state conditions following each chemical addition. Protein content was analyzed using the Bradford technique (Bradford, 1976).

Enzyme activities. Citrate synthase (CS) and ETS complex maximal activities (V_{max}) were assessed using spectrophotometric biochemical assays from whole brain, as described previously (Galli et al., 2013).

H^+ leak measurements. H^+ flux kinetics across the inner mitochondrial membrane were assessed by simultaneous measurement of O_2 consumption and H^+-motive force, in the presence of succinate and oligomycin, using tetraphenylphosphonium (TPP^+), as described previously (Galli et al., 2013) and using an O2k TPP^+ ion selective electrode (Oroboros). Note that this methodology excludes any contribution of ΔpH and therefore resulting measurements of the H^+-motive force are likely slight

underestimates of the true value. Mitochondrial matrix volume was not measured because changes in this parameter have minimal impact on TPP-mediated measurements of $\Delta\Psi_m$ (Rottenberg, 1984). We employed a binding factor b for mitochondria of 0.16 (Marcinkeviciute et al., 2000; Galli et al., 2013). The kinetics of H^+ flux were determined by inhibiting the substrate oxidation component by stepwise addition of 0.5 or 1.0 µl aliquots of malonate (2.0 M stock) and measuring the effect on $\Delta\Psi_m$. After the final malonate addition, carbonyl cyanide p-trifluoro-methoxyphenylhydrazone (FCCP, 1 µM) was added to uncouple mitochondria and determine the degree of electrode drift. H^+ flux curves were fit using a two-parameter exponential growth curve.

Statistics. Statistical analysis was performed using commercial software (SPSS 15.0, SPSS Inc., Chicago, IL). For all experiments, individual *n* values correspond to a single animal. Values are presented as mean ± SEM. All data were normally distributed with equal variance ($P > 0.05$). For all data, significance was evaluated using a repeated-measures 2-way ANOVA to test for significant interactions between the two independent variables: (*i*) the substrate or inhibitor injected (*e.g.* ADP vs. succinate), and (*ii*) inhaled O_2 level (normoxia and hypoxia). Bonferonni post hoc multiple comparisons tests were run on each of the dependent variables to compare the single point means of interest. $P < 0.05$ was considered to achieve statistical significance unless otherwise indicated.

Results

Whole animal oxygen consumption rate and mitochondrial ETS flux are markedly reduced by acute hypoxia. The whole animal oxygen consumption rate of NMRs in normoxia was ~ 40 ml O_2•min•kg^{-1} throughout 7 hours of measurement (n = 10; Fig. 1, open circles), consistent with previous reports of normoxic metabolic rates in this species (Buffenstein, 1996; Pamenter et al., 2015; Chung et al., 2016). Conversely, in acute hypoxia (4 hours at 3% O_2), the NMR whole-organism oxygen consumption rate decreased by ~ 85% (from 41.6 ± 5.8 to 6.1 ± 3.0 ml O_2•min•kg^{-1}, n = 6, Fig. 1, squares) and recovered to pre-treatment levels within 2 hours of reoxygenation (36.8 ± 7.2 ml O_2•min•kg^{-1}, n = 4, Fig. 1).

We next examined mitochondrial respiratory flux in permeabilized brain from normoxic control and acutely hypoxic NMRs using a SUIT protocol. In permeabilized brain isolated from hypoxia-treated NMRs, respiratory flux through the entire ETS was decreased relative to permeabilized brain from normoxic NMRs (Fig. 2A). Specifically, a 2-way repeated measures ANOVA revealed a significant treatment effect between normoxia and hypoxia on ETS respiratory flux. Further analysis with Bonferonni posthoc tests revealed specific changes in state II (pyruvate (5.0 mM final concentration; 5.0 µl of 2.0 M stock), malate (2.0 mM final concentration; 5.0 µl of 0.8M stock) and glutamate (10.0 mM final concentration; 10.0 µl of 2.0 M stock)-fueled) and III (pyruvate, malate, glutamate, and ADP (1.5 mM final concentration; 6 µl of 0.5 M stock)-fueled) mitochondrial respiration rates, which were 84 and 54% lower, respectively, in permeabilized brain from NMRs exposed to acute hypoxia than from controls (Fig. 2A). Measurements of respiration through the individual components of the ETS revealed that the activity of complexes I, II, and IV decreased by 77, 53, and 64%, respectively in hypoxic brain (Fig. 2A). As a result of this consistent downregulation of the ETS, total ETS capacity (as indicated by complex I and II fueled, FCCP-uncoupled respiration rates) was drastically reduced by 88% following acute *in vivo* hypoxia (Fig.

2B). Relative to FCCP-uncoupled respiration, only complex IV (cytochrome c oxidase: COX)-fueled respiration (stimulated by TMPD and ascorbate) was modified by the low O_2 challenge (Fig. 2C), suggesting a regulatory role for this enzyme in this response.

ETS complex enzyme activity is unaltered by acute hypoxia. CS V_{Max} was unchanged between treatments (Fig. 3A). Similarly, the V_{max} of ETS complexes I-V were unaltered by acute hypoxia (Fig. 3B).

NMR permeabilized brain has lower H^+ leak and a respiration rate following acute hypoxia. Next we compared kinetics of the mitochondrial H^+ gradient between treatment groups (Fig. 4). A 2-way repeated measures ANOVA revealed that mitochondria from hypoxia-treated NMR permeabilized brain had lower rates of O_2 consumption and a more depolarized $\Delta\Psi_m$ than mitochondria from control animals. Specifically, State II respiration rate (in the presence of succinate (10 mM final concentration; 20.0 µl of 1.0 M stock) and oligomycin) at the start of the experiment of permeabilized brain from hypoxic NMRs was reduced by ~ 50% relative to untreated controls, and $\Delta\Psi_m$ was markedly decreased by ~ 25 mV at each data point. For example, when H^+ leak kinetics were considered at a common $\Delta\Psi_m$ of 110 mV, hypoxic NMR permeabilized brain H^+ leak was ~ ½ that of normoxic NMR permeabilized brain (Fig. 4B). Conversely, the rates of both respiration rate and $\Delta\Psi_m$ discharge with malonate additions were similar between treatments (Figs. 4C&D), and the kinetic relationship between respiratory flux and $\Delta\Psi_m$ with titrated additions of malonate was not different between treatment groups as assessed using two-parameter exponential growth curves.

Discussion

We explored the effect of acute hypoxia on the functional characteristics of hypoxia-tolerant NMR brain mitochondria. To our knowledge, our study is the first to examine any aspect of mitochondrial function in NMR brain. Our study yielded two important findings. First, NMRs markedly decrease their oxygen consumption rate by ~ 85% during prolonged severe hypoxia. Second, in hypoxic NMR brain, ETS respiration and H^+ leak are markedly reduced, suggesting a reduced need for aerobically generated ATP during hypoxia. Taken together, these results support our hypotheses that NMR brain mitochondria exhibit functional plasticity and contribute to profound whole-animal metabolic rate suppression during acute *in vivo* hypoxic exposure in this species.

A handful of studies have explored the function of mitochondria in lowland hypoxia-tolerant species and our data agree well with these previous studies. Indeed, although the effect of adaptation through multiple generations of hypoxia-acclimation on mitochondrial respiratory flux is not well understood, there is a strong consensus that acute or prolonged hypoxic exposure exerts consistent inhibitory effects on mitochondrial respiration rates in hypoxia-tolerant lowland species. For example: *i*) states III and IV respiration are lower in gill mitochondria of intertidal pacific oysters [*Crassostrea gigas*] following both 3 and 12 hrs of hypoxia (Sussarellu et al., 2013), *ii*) state II, III, and IV respiration are lower, following 2 weeks of anoxic exposure, in the brain of the anoxia-tolerant freshwater turtle [*Trachemys scripta*], due in part to an ~ 50% reduction in complex I activity (Pamenter et al., 2016), while *iii*), state III respiration is lower due to reductions in complex I and IV activity in hearts of the same species (Galli et al., 2013). Similarly, *iv*) states III and IV respiration rates are 20-30% lower in skeletal muscle mitochondria isolated from hypoxia-tolerant frogs [*Rana temporaria*] following exposure to 1 or 4 months of hypoxia (St-Pierre et al., 2000), and *v*) in *Drosophila melanogastor* that had been raised under chronic hypoxia (4% O_2) for

> 200 generations, state III respiration was lower relative to naïve flies, due primarily to reduced complex II activity (Ali et al., 2012).

An important caveat of these previous studies and also of our current results is that mitochondrial isolation procedures, for both permeabilized cells and also isolated mitochondria, are commonly conducted in standard laboratory atmospheric conditions. As a result, and depending on the isolation protocol, tissues from animals exposed to hypoxia *in vivo* are thus incubated in normoxia for 1-3 hrs prior to experimentation. However, despite this potentially confounding factor, it is nonetheless notable that mitochondria from normoxia- and hypoxia-treated NMRs exhibit drastically different ETS respiratory flux rates, despite being isolated identically *ex vivo*. These functional differences indicate that the *in vivo* hypoxic exposure had long lasting effects on mitochondrial function. Similarly rapid responses have been reported in other organisms exposed to short-term hypoxia (Sussarellu et al., 2013). The underlying effectors of these changes are unknown but may involve rapid mechanisms such as post-translational modifications (Stram and Payne, 2016). In particular, redox-related modifications of mitochondrial proteins are a rapidly inducible mechanism to inhibit ETS complexes (Kramer et al., 2015); redox signaling is typically altered by changes in oxygen availability and thus is a good candidate for further studies to elucidate the mechanisms underlying the rapid and sustained down-regulation of mitochondrial function.

Notably, similar adaptive responses have been reported in hypoxia-intolerant species acclimated to chronic hypoxia. For example: *vi*) state II and IV respiration and complexes I and IV activity are all reduced in mouse brain mitochondria following exposure to chronic hypoxia for 21 days (Chavez et al., 1995), and *vii*) state III respiration and complex I and II flux rates are lower in skeletal muscle mitochondria of humans acclimated for 4 weeks at altitude relative to pre-acclimatization rates in the same individuals (Jacobs et al., 2012). Such examples of reduced ETS flux as an adaptation to hypoxia in low altitude species are likely associated with reduced metabolic

requirements during hypoxic challenges. Indeed, reducing metabolic demand when O_2 is limiting, particularly in brain tissue, is a common strategy employed by hypoxia-tolerant and hypoxia-adapted species (Hochachka et al., 1996; Buck and Pamenter, 2006), including human populations that have lived at altitude for 1000's of years (Hochachka et al., 1994). This relationship holds true in our analysis of the effects of acute hypoxia on NMR mitochondrial function.

Interestingly, an opposing phenotype is reported in several studies of high altitude species that inhabit niches in which hypobaric hypoxia is compounded by a cold environment. For example, high altitude populations of the Andean torrent duck [*Merganetta armata*] exhibit heightened respiratory capacities in gastrocnemius muscle, which is the primary muscle used for swimming and diving behaviors in this species (Dawson et al., 2016). Similarly, high altitude deer mice [*Peromyscus maniculatus*] also exhibit higher respiratory capacities in their gastrocnemius muscle mitochondria and also higher mitochondrial volume densities relative to those of low altitude populations of deer mice (Mahalingam et al., 2017). Conversely, in flight muscles of bar-headed geese [*Anser indicus*] and Tibetan locusts [*Locusta migratoria*], two species adapted to living and exercising at high altitude for 1000's of years, mitochondrial respiratory flux is not different from that of mitochondria isolated from flight muscles of lowland species of geese and locusts, respectively (Zhang et al., 2013; Scott et al., 2015). It should be noted, however, that bar-headed geese face a unique exercise challenge in that they increase their O_2 consumption by 10 to 20-fold while in hypoxia to sustain flight activities at high altitudes, and thus exhibit a remarkable suite of unique adaptive strategies that are difficult to compare directly to other hypoxia-adapted or –acclimated species that do not face a similarly extreme exercise challenge while in hypoxia. Similarly, high-altitude species face a significant thermoregulatory challenge due to the cold climate at altitude and this has a significant impact on mitochondrial physiology. Therefore, high-altitude denizens face a unique set of trade-offs between hypoxia-tolerance and thermoregulation

that confound determination of an optimal phenotype to enhance mitochondrial function in hypoxia. This compounded ecophysiological stress has likely applied different evolutionary pressures to this species than those applied to lowland species that do not face the same degree of thermoregulatory challenge in their natural environment.

COX activity is reduced in hypoxic NMR brain mitochondria. An important observation of our study is that NMR oxygen consumption rate was > 85% reduced in acute hypoxia; permeabilized brain from these animals exhibited drastically lower rates of O_2 consumption and a more depolarized $\Delta\Psi_m$ than control animals. Intriguingly, when normalized to FCCP-uncoupled respiration, only complex IV fueled respiration (stimulated by TMPD and ascorbate) was modified by the low O_2 challenge (Fig. 2C), suggesting a regulatory role for this enzyme in this response. COX is the terminal complex of the ETS and is the major site via which O_2 interacts with the ETS. Therefore, COX is ideally positioned to serve as a regulator of ETS flux in acute hypoxia and in rat hepatocytes, reduced ETS respiratory flux during acute hypoxia is triggered by a regulatory effect of molecular O_2 on COX (Chandel et al., 1995). Our observation of reduced COX activity relative to total ETS capacity in hypoxia-treated NMR brain is consistent with examinations of skeletal muscle mitochondria from other hypoxia-tolerant species (Scott et al., 2011; Zhang et al., 2013), and may be due to an upregulation of COX isoform IV-2 in astrocytes and cerebellar granule cells following acute hypoxia in brain (Horvat et al., 2006). In this study, the authors reported that in murine brain cells, *in vitro* exposure to a few hours of hypoxia elevated COX isoform IV-2, which in turn abolished the allosteric inhibition of COX by ATP. This finding indicates that COX may function as an oxygen sensor in mammal brain and can directly modulate ETS function. The rapid mode of action observed in our study suggests that COX may modify ETS function via a similar rapid cellular signaling process in NMRs. Further studies are warranted to examine this hypothesis.

Conclusions. Mitochondria are the nexus of O_2 consumption and metabolism in the cell, and also coordinate deleterious and neuroprotective responses to low O_2 stress (Pamenter, 2014). NMRs have a low basal metabolic rate and we demonstrate here that they exhibit metabolic arrest in acute hypoxia. The degree to which NMRs are able to decrease their oxygen consumption rate in hypoxia is unprecedented in awake and active mammals. It is notable that the drastic reduction in ETS flux is similar to the magnitude of the reduction in whole animal oxygen consumption rate observed in this species during the same period of acute hypoxia and no doubt contributes to this species' ability to suppress metabolic demand in low O_2 conditions. Reducing metabolic rate when O_2 is limiting, particularly in brain tissue, is a common strategy employed by hypoxia-tolerant species (Buck and Pamenter, 2006), and this relationship holds true in our analysis of NMR whole animal oxygen consuption rate and mitochondrial function during acute hypoxia.

In general, our findings support an emerging consensus in the literature concerning the effects of acute hypoxia exposure on mitochondrial adaptations, at least as this pertains to low-altitude species. The available evidence suggests that common adaptations to hypoxia at low altitude include functional remodeling of mitochondrial metabolism in hypoxia-tolerant and -intolerant species. This remodeling is characterized by some or all of a number of hallmarks, including: decreased overall ETS flux, reductions in mitochondrial volume density, and changes in COX activity and kinetics. Our findings regarding the function of brain mitochondria from hypoxia-tolerant NMRs fit this paradigm. Specifically, NMR brain tissue exhibits rapid plasticity in acute hypoxia including large-scale reductions in brain mitochondrial respiration and the H^+ gradient. We conclude that NMR brain mitochondrial metabolism is primed to maximize energetic efficiency and support marked and rapid reductions in whole oxygen consumption rate during hypoxia.

Funding

This work was supported by an NSERC Discovery grant to WKM and a Parker B Francis PDF to MEP.

Data Accessibility

Supporting data will be uploaded to Dryad in keeping with the journal's policies.

Competing Interests

We have no competing interests.

Author Contributions

MEP conceived of and designed the study and wrote the manuscript. MEP performed the whole animal respirometry experiments and the high-resolution respirometry experiments. GYL performed the molecular biology experiments and MEP and GYL analyzed data. All authors contributed to the experimental design, edited the manuscript, and gave final approval for the published version, and agree to be accountable for all content therein.

References

Ali, S. S., Hsiao, M., Zhao, H. W., Dugan, L. L., Haddad, G. G. and Zhou, D. (2012). Hypoxia-adaptation involves mitochondrial metabolic depression and decreased ROS leakage. *PLoS One* **7**, e36801.

Bradford, M. M. (1976). A rapid and sensitive method for the quantitation of microgram quantities of protein utilizing the principle of protein-dye binding. *Anal Biochem* **72**, 248-254.

Brett, R. A. (1991). The Population Structure of Naked Mole-Rat Colonies. In *The Biology of the Naked Mole-Rat*, eds. P. W. Sherman J. U. Jarvis and R. D. Alexander), pp. 97-136. Princeton: Princeton University Press.

Buck, L. T. and Pamenter, M. E. (2006). Adaptive responses of vertebrate neurons to anoxia-Matching supply to demand. *Respir Physiol Neurobiol* **154**, 226-240.

Buffenstein, R. (1996). Ecophysiological responses to a subterranean habitat; A Bathyergid perspective. *Mammalia* **60**, 591-605.

Chandel, N., Budinger, G. R., Kemp, R. A. and Schumacker, P. T. (1995). Inhibition of cytochrome-c oxidase activity during prolonged hypoxia. *Am J Physiol* **268**, L918-925.

Chavez, J. C., Pichiule, P., Boero, J. and Arregui, A. (1995). Reduced mitochondrial respiration in mouse cerebral cortex during chronic hypoxia. *Neurosci Lett* **193**, 169-172.

Choi, D. W. (1992). Excitotoxic cell death. *J Neurobiol* **23**, 1261-1276.

Chung, D., Dzal, Y. A., Seow, A., Milsom, W. K. and Pamenter, M. E. (2016). Naked mole rats exhibit metabolic but not ventilatory plasticity following chronic sustained hypoxia. *Proc Biol Sci* **283**.

Dawson, N. J., Ivy, C. M., Alza, L., Cheek, R., York, J. M., Chua, B., Milsom, W. K., McCracken, K. G. and Scott, G. R. (2016). Mitochondrial physiology in the skeletal and cardiac muscles is altered in torrent ducks, *Merganetta armata*, from high altitudes in the Andes. *Journal of Experimental Biology* **219**, 3719-3728.

Galli, G. L., Lau, G. Y. and Richards, J. G. (2013). Beating oxygen: chronic anoxia exposure reduces mitochondrial F1FO-ATPase activity in turtle (*Trachemys scripta*) heart. *J Exp Biol* **216**, 3283-3293.

Hochachka, P. W., Buck, L. T., Doll, C. J. and Land, S. C. (1996). Unifying theory of hypoxia tolerance: molecular/metabolic defense and rescue mechanisms for surviving oxygen lack. *Proc Natl Acad Sci U S A* **93**, 9493-9498.

Hochachka, P. W., Clark, C. M., Brown, W. D., Stanley, C., Stone, C. K., Nickles, R. J., Zhu, G. G., Allen, P. S. and Holden, J. E. (1994). The brain at high altitude: hypometabolism as a defense against chronic hypoxia? *J Cereb Blood Flow Metab* **14**, 671-679.

Hogg, D. W., Pamenter, M. E., Dukoff, D. J. and Buck, L. T. (2015). Decreases in mitochondrial reactive oxygen species initiate GABA(A) receptor-mediated electrical suppression in anoxia-tolerant turtle neurons. *J Physiol* **593**, 2311-2326.

Holtze, S., Eldarov, C. M., Vays, V. B., Vangeli, I. M., Vysokikh, M. Y., Bakeeva, L. E., Skulachev, V. P. and Hildebrandt, T. B. (2016). Study of age-dependent structural and functional changes of mitochondria in skeletal muscles and heart of naked mole rats (*Heterocephalus glaber*). *Biochemistry (Mosc)* **81**, 1429-1437.

Horvat, S., Beyer, C. and Arnold, S. (2006). Effect of hypoxia on the transcription pattern of subunit isoforms and the kinetics of cytochrome c oxidase in cortical astrocytes and cerebellar neurons. *Journal of Neurochemistry* **99**, 937-951.

Jacobs, R. A., Siebenmann, C., Hug, M., Toigo, M., Meinild, A. K. and Lundby, C. (2012). Twenty-eight days at 3454-m altitude diminishes respiratory capacity but enhances efficiency in human skeletal muscle mitochondria. *FASEB J* **26**, 5192-5200.
Johansen, K., Lykkeboe, G., Weber, R. E. and Maloiy, G. M. (1976). Blood respiratory properties in the naked mole rat *Heterocephalus glaber*, a mammal of low body temperature. *Respir Physiol* **28**, 303-314.
Kirby, A. M., Fairman, G. and Pamenter, M. E. (In revision). Atypical behavioural, metabolic, and thermoregulatory responses to hypoxia in the naked mole rat (Heterocephalus glaber). *J Zool* **In revision**.
Kramer, P. A., Duan, J. C., Qian, W. J. and Marcinek, D. J. (2015). The Measurement of Reversible Redox Dependent Post-translational Modifications and Their Regulation of Mitochondrial and Skeletal Muscle Function. *Frontiers in Physiology* **6**.
Mahalingam, S., McClelland, G. B. and Scott, G. R. (2017). Evolved changes in the intracellular distribution and physiology of muscle mitochondria in high-altitude native deer mice. *J Physiol-London* **595**, 4785-4801.
Marcinkeviciute, A., Mildaziene, V., Crumm, S., Demin, O., Hoek, J. B. and Kholodenko, B. (2000). Kinetics and control of oxidative phosphorylation in rat liver mitochondria after chronic ethanol feeding. *Biochem J* **349**, 519-526.
Nathaniel, T. I., Saras, A., Umesiri, F. E. and Olajuyigbe, F. (2009). Tolerance to oxygen nutrient deprivation in the hippocampal slices of the naked mole rats. *J Integr Neurosci* **8**, 123-136.
Pamenter, M. E. (2014). Mitochondria: a multimodal hub of hypoxia tolerance. *Can J Zool* **92**, 569-589.
Pamenter, M. E., Richards, M. D. and Buck, L. T. (2007). Anoxia-induced changes in reactive oxygen species and cyclic nucleotides in the painted turtle. *J Comp Physiol [B]* **177**, 473-481.
Pamenter, M. E., Dzal, Y. A. and Milsom, W. K. (2014). Profound metabolic depression in the hypoxia-tolerant naked mole rat. *FASEB J* **28**, 879.872.
Pamenter, M. E., Dzal, Y. A. and Milsom, W. K. (2015). Adenosine receptors mediate the hypoxic ventilatory response but not the hypoxic metabolic response in the naked mole rat during acute hypoxia. *Proc Biol Sci* **282**, 20141722.
Pamenter, M. E., Shin, D. S., Cooray, M. and Buck, L. T. (2008). Mitochondrial ATP-sensitive K+ channels regulate NMDAR activity in the cortex of the anoxic western painted turtle. *J Physiol* **586**, 1043-1058.
Pamenter, M. E., Gomez, C. R., Richards, J. G. and Milsom, W. K. (2016). Mitochondrial responses to prolonged anoxia in brain of red-eared slider turtles. *Biology letters* **12**.
Pamenter, M. E., Hogg, D. W., Ormond, J., Shin, D. S., Woodin, M. A. and Buck, L. T. (2011). Endogenous GABA(A) and GABA(B) receptor-mediated electrical suppression is critical to neuronal anoxia tolerance. *Proc Natl Acad Sci U S A* **108**, 11274-11279.
Pamenter, M. E., Ali, S. S., Tang, Q., Finley, J. C., Gu, X. Q., Dugan, L. L. and Haddad, G. G. (2012). An in vitro ischemic penumbral mimic perfusate increases NADPH oxidase-mediated superoxide production in cultured hippocampal neurons. *Brain Res* **1452**, 165-172.
Park, T. J., Reznick, J., Peterson, B. L., Blass, G., Omerbasic, D., Bennett, N. C., Kuich, P., Zasada, C., Browe, B. M., Hamann, W. et al. (2017). Fructose-driven glycolysis supports anoxia resistance in the naked mole-rat. *Science* **356**, 307-311.
Peterson, B. L., Park, T. J. and Larson, J. (2012). Adult naked mole-rat brain retains the NMDA receptor subunit GluN2D associated with hypoxia tolerance in neonatal mammals. *Neurosci Lett* **506**, 342-345.

Rottenberg, H. (1984). Membrane potential and surface potential in mitochondria: uptake and binding of lipophilic cations. *J Membr Biol* **81**, 127-138.
Scott, G. R., Schulte, P. M., Egginton, S., Scott, A. L., Richards, J. G. and Milsom, W. K. (2011). Molecular evolution of cytochrome C oxidase underlies high-altitude adaptation in the bar-headed goose. *Mol Biol Evol* **28**, 351-363.
Scott, G. R., Hawkes, L. A., Frappell, P. B., Butler, P. J., Bishop, C. M. and Milsom, W. K. (2015). How bar-headed geese fly over the Himalayas. *Physiology (Bethesda)* **30**, 107-115.
St-Pierre, J., Tattersall, G. J. and Boutilier, R. G. (2000). Metabolic depression and enhanced O(2) affinity of mitochondria in hypoxic hypometabolism. *Am J Physiol Regul Integr Comp Physiol* **279**, R1205-1214.
Stoll, E. A., Karapavlovic, N., Rosa, H., Woodmass, M., Rygiel, K., White, K., Turnbull, D. M. and Faulkes, C. G. (2016). Naked mole-rats maintain healthy skeletal muscle and Complex IV mitochondrial enzyme function into old age. *Aging-Us* **8**, 3468-+.
Stram, A. R. and Payne, R. M. (2016). Post-translational modifications in mitochondria: protein signaling in the powerhouse. *Cell Mol Life Sci* **73**, 4063-4073.
Sussarellu, R., Dudognon, T., Fabioux, C., Soudant, P., Moraga, D. and Kraffe, E. (2013). Rapid mitochondrial adjustments in response to short-term hypoxia and re-oxygenation in the Pacific oyster, *Crassostrea gigas*. *J Exp Biol* **216**, 1561-1569.
Zhang, Z. Y., Chen, B., Zhao, D. J. and Kang, L. (2013). Functional modulation of mitochondrial cytochrome c oxidase underlies adaptation to high-altitude hypoxia in a Tibetan migratory locust. *Proc Biol Sci* **280**, 20122758.

Figures

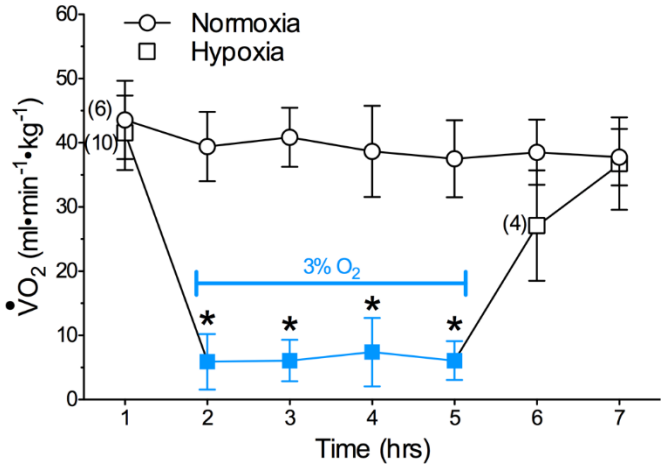

Figure 1. NMR whole-animal oxygen consumption rate is markedly decreased in acute hypoxia. Oxygen consuption rates of individual NMRs exposed to normoxia (21% O_2, open circles) and then 4 hrs of hypoxia (3% O_2, blue squares). Data are mean ± SEM. Numbers in parenthesis indicate *n*. Asterisks (*) indicate significant difference from normoxic controls ($p < 0.05$; 2-way RM ANOVA).

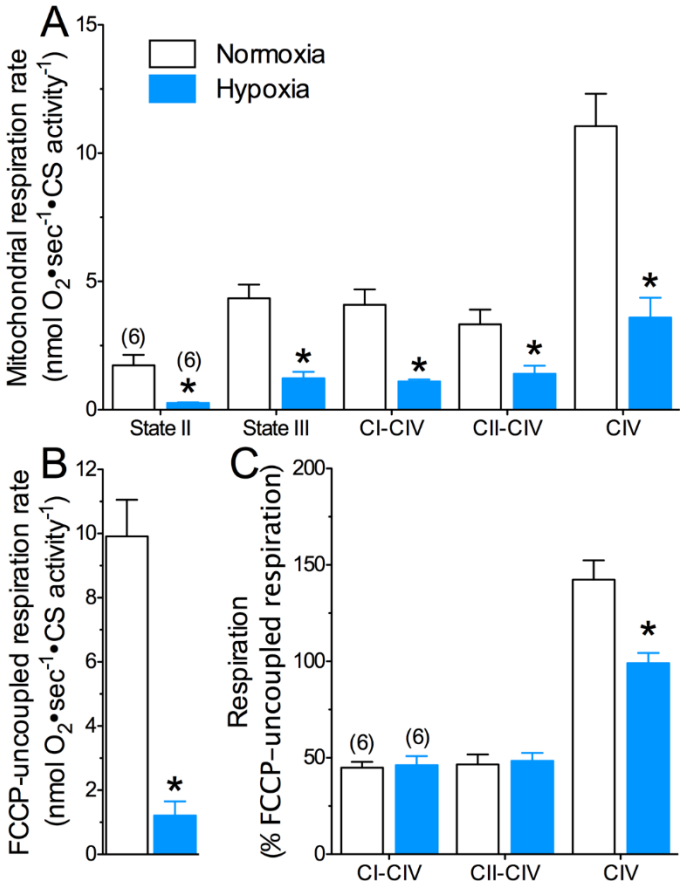

Figure 2. NMR brain mitochondria exhibit functional plasticity following *in vivo* exposure to 4 hrs of hypoxia (3% O_2). (A) Individual complex respiratory rates from animals exposed to normoxia (white bars) or acute hypoxia (blue bars). **(B)** Comparison of complex I and II fueled FCCP-uncoupled respiration rates. **(C)** Summary of ETS complex respiration rates normalized to FCCP-uncoupled maximum respiration. Data are mean ± SEM. Numbers in parenthesis indicate *n*. Asterisks (*) indicate significant differences between mice and naked mole rat mitochondria ($p < 0.05$; 2-way RM ANOVA).

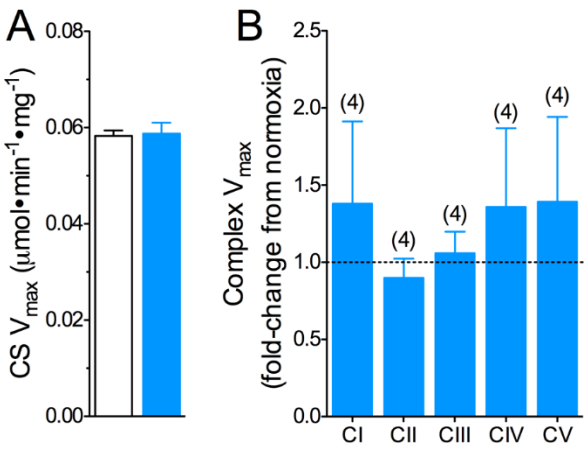

Figure 3. Complex enzyme maximum activity is not altered by acute hypoxia. (A) Summary of citrate synthase (CS) V_{max} in normoxic (white bars) and acutely hypoxic NMRs (blue bars). **(B)** Summary of electron transport system (ETS) complexes I-V activity from acutely hypoxic NMR brain tissue normalized to ETS complex activity from normoxic control NMR brain tissue. Data are mean ± SEM. Numbers in parenthesis indicate *n*. ($p < 0.05$; 2-way RM ANOVA).

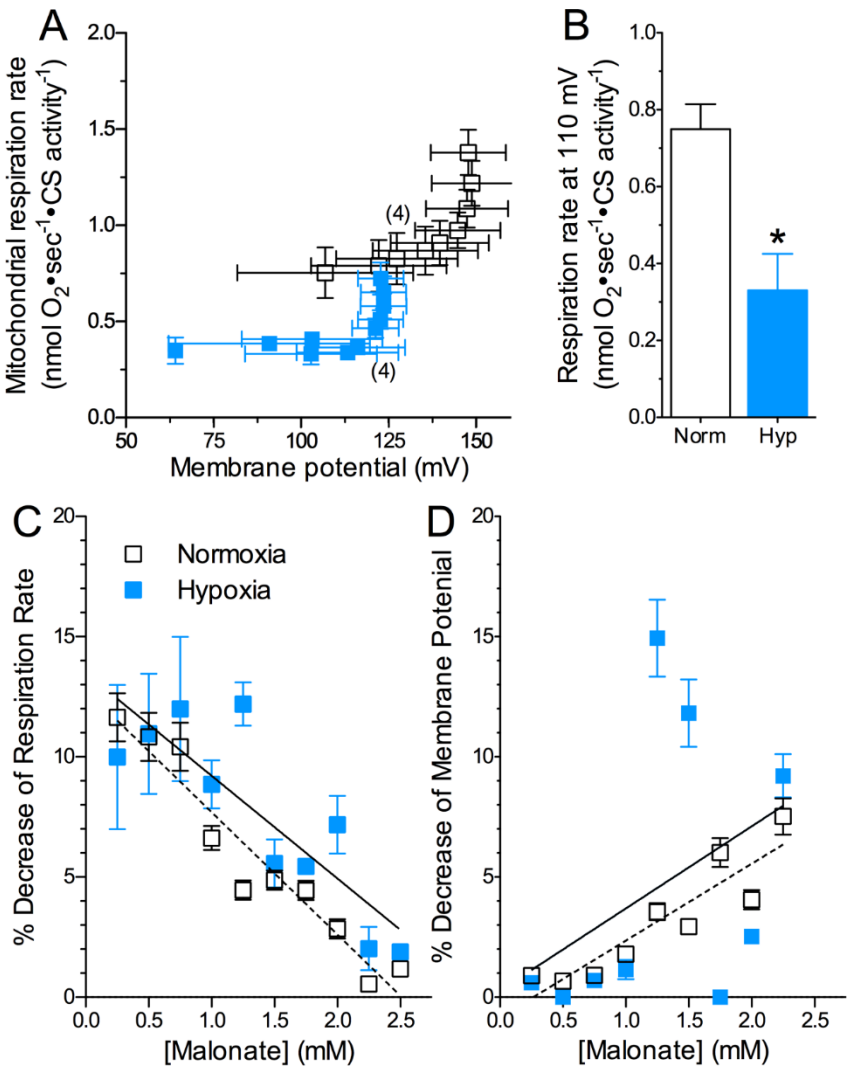

Figure 4. The mitochondrial H^+ gradient of NMR brain mitochondria is reduced relative to normoxic control animals. (A) Hypoxic NMR (blue squares) brain H^+ flux and O_2 consumption are equally coupled but reduced in magnitude relative to normoxic control NMR brain (open squares). **(B)** Comparison of H^+ flux rates at a common mitochondrial membrane potential of 110 mV. **(C)** Percent decrease of mitochondrial respiration and **(D)** mitochondrial membrane potential with step-wise addition of malonate. Data are mean ± SEM. Numbers in parenthesis indicate *n*. Asterisks (*) indicate significant differences between mice and NMR mitochondria ($p < 0.05$; 2-way RM ANOVA).